


p16^{Ink4a}, a marker of cellular senescence, is associated with renal disease in the B6.NZMSle1/Sle2/Sle3 mouse model of lupus

Gaëlle Tilman,^{1,2} Emilie Dupré,¹ Laura Watteyne,¹ Charlotte Anne Baert,¹ Delphine Nolf,¹ Fatima Benhaddi,¹ Fanny Lambert,¹ Aurélie Daumerie,³ Caroline Bouzin,³ Sophie Lucas,¹ Nisha Limaye ¹

To cite: Tilman G, Dupré E, Watteyne L, *et al.* p16^{Ink4a}, a marker of cellular senescence, is associated with renal disease in the B6.NZMSle1/Sle2/Sle3 mouse model of lupus. *Lupus Science & Medicine* 2023;**10**:e001010. doi:10.1136/lupus-2023-001010

► Additional supplemental material is published online only. To view, please visit the journal online (<http://dx.doi.org/10.1136/lupus-2023-001010>).

GT and ED contributed equally.

Received 1 August 2023
Accepted 9 October 2023



© Author(s) (or their employer(s)) 2023. Re-use permitted under CC BY-NC. No commercial re-use. See rights and permissions. Published by BMJ.

¹de Duve Institute, Université catholique de Louvain, Brussels, Belgium

²Department of Rheumatology, Cliniques universitaires Saint-Luc, Brussels, Belgium

³REC Imaging Platform (2IP), Institut de Recherche Expérimentale et Clinique, Université catholique de Louvain, Brussels, Belgium

Correspondence to

Dr Nisha Limaye; nisha.limaye@uclouvain.be

ABSTRACT

Objectives Despite treatment, one-third of patients with lupus nephritis (LN) show a decline in renal function. Prognostic markers of poor outcome as well as novel therapeutic targets are therefore highly sought. We showed that p16^{Ink4a}, a marker of cellular senescence, is observed in baseline kidney biopsies from patients with LN, and is associated with renal disease. Here, we set out to assess for whether these findings are recapitulated in the B6.NZMSle1/Sle2/Sle3 (B6.Sle1.2.3) mouse model of spontaneous lupus.

Methods We evaluated the occurrence and time of onset of p16^{Ink4a} staining by immunohistochemistry on kidney sections, and tested for its association with multiple renal and systemic disease parameters, fibrosis and CD8⁺ T cell infiltration, in two cohorts of B6.Sle1.2.3 mice.

Results The presence of p16^{Ink4a}-positive cells in kidney was significantly associated with increased urine albumin/creatinine ratio, histopathological scores, CD8⁺ T cell infiltration and fibrosis, in both B6.Sle1.2.3 cohorts. In contrast, p16^{Ink4a} staining was not associated with systemic disease parameters. A time course showed that systemic disease parameters as well as glomerular IgG deposits appeared in B6.Sle1.2.3 mice by 4 months of age; the appearance of p16^{Ink4a}-positive cells occurred later, by 8 months of age, overlapping with renal disease.

Conclusion We report, for the first time, the presence of p16^{Ink4a}-positive cells, a marker of cellular senescence, in the B6.Sle1.2.3 kidney, and their association with renal disease severity. This provides a preclinical model in which to test for the role of cellular senescence in the pathogenesis of LN, as a potential kidney-intrinsic disease mechanism.

INTRODUCTION

Lupus nephritis (LN) is a frequent, serious complication of SLE. It is considered an immune complex-mediated disease, initiated by anti-double-stranded DNA (anti-dsDNA) antibody deposition in glomerular basement membranes, causing complement activation and immune cell recruitment, ultimately

WHAT IS ALREADY KNOWN ON THIS TOPIC

⇒ p16^{Ink4a} staining (a classic marker of cellular senescence) in baseline kidney biopsies from patients with lupus nephritis (LN) is associated with higher histopathological scores, as well as impairment of kidney function at baseline and 5 years post-treatment initiation. Senescence-associated β-galactosidase staining (another classic marker) in kidneys is associated with proteinuria in MRL/lpr mice that develop a strong autoimmune phenotype due to a *Fas* gene mutation.

WHAT THIS STUDY ADDS

⇒ We show that p16^{Ink4a} staining is observed in kidneys of B6.NZMSle1/Sle2/Sle3 lupus-prone mice; as in patients, it is associated with multiple renal (but not systemic) disease parameters. A time course experiment showed that p16^{Ink4a} staining is observed by 8 months of age, overlapping with renal disease onset and well after systemic disease onset (by 2–4 months of age) in this model.

HOW THIS STUDY MIGHT AFFECT RESEARCH, PRACTICE OR POLICY

⇒ The detection and targeting of senescent renal cells may be useful in LN management. This study provides a preclinical model for the testing of senolytic drugs (that target senescent cells), and an alternative source (besides kidney biopsies from patients with LN) of cells for in vitro mechanistic studies of the interactions between senescent renal cells and immune cells.

leading to renal injury and loss of kidney function.^{1,2} Although initial triggering events are well characterised, intrarenal mechanisms of progression remain poorly understood, and may reveal novel biomarkers and therapeutic targets. A significant fraction of patients fails to respond adequately to standard therapies of high-dose corticosteroids and other immunosuppressive agents; 5–10% develop end-stage renal disease within 10 years of disease

onset.³ Neither histopathological (International Society of Nephrology and Renal Pathology Society) classification of baseline kidney biopsy (the gold standard for diagnosis and therapeutic decision-making), nor persistent proteinuria (the current gold-standard marker of disease activity) predicts poor outcome sufficiently well.^{4–6} The identification of markers for patients at high risk of poor outcome, who might benefit from appropriately tailored therapy, is therefore an urgent unmet need in the field.

We previously showed that the presence of p16^{INK4a}-positive cells (a marker of cellular senescence) in baseline kidney biopsies of patients with LN was significantly associated with renal disease, both at baseline and 5 years post-treatment initiation.⁷ Intriguingly, glomerular p16^{INK4a}-positive renal cells displayed significant spatial co-distribution with infiltrating periglomerular CD8⁺ T cells and fibrosis.⁷ Cellular senescence, triggered by stressors such as telomere erosion, genotoxic and oxidative stress, oncogene activation and inflammatory cytokines, leads to irreversible cell cycle arrest through the accumulation of cyclin-dependent kinase (CDK) inhibitors such as p16^{INK4a} (*CDKN2A*).^{8–10} Senescent cells nevertheless remain metabolically active and undergo morphological and physiological changes including the upregulation of β -galactosidase activity and the acquisition of a proinflammatory, profibrotic senescence-associated secretory phenotype (SASP).^{11–13} The SASP is adept at engaging the immune system, with macrophages, natural killer, CD4⁺ T helper, as well as, more recently, CD8⁺ T cells described to mediate clearance of senescent cells.^{14–19}

The accumulation of senescence markers has been reported in renal ageing and disease, and is associated with histological and clinical signs of renal impairment.^{20–25} The presence of β -galactosidase-positive cells in kidneys was observed to correlate with α -SMA expression and proteinuria in MRL/*lpr* mice.²⁶ These mice develop lupus-like autoimmunity due to a *Fas* gene mutation; in humans, *FAS* mutations cause a distinct disorder: autosomal dominant autoimmune lymphoproliferative syndrome (type IA; MIM# 601859).^{27–29} Here, we assess for the presence and time of onset of renal cell senescence in the B6.NZM*Sle1/Sle2/Sle3* (B6.*Sle1.2.3*) congenic mouse strain. This inbred strain contains three susceptibility loci for SLE from the NZM2410 lupus-prone strain, on the C57BL/6 (B6) genetic background: *Sle1* (located on chromosome 1) is responsible for a break in tolerance to nuclear antigens,³⁰ *Sle2* (on chromosome 4) leads to B cell hyperactivity,³¹ and *Sle3* (on chromosome 7) induces hyperstimulation of antigen presenting cells and a dysregulation of CD4⁺ T cells.³² Together, they cause a highly penetrant and severe lupus phenotype that greatly resembles that in humans, by 12 months of age.³³

METHODS

Mice

B6 and B6.*Sle1.2.3* mice were bred and maintained in the SPF animal facility of the university. Plasma (from

retro-orbital blood), urine and kidneys (cut in half longitudinally, for formalin-fixed paraffin-embedded (FFPE) and optimal cutting temperature (OCT)-embedded blocks) were collected from two cohorts of mice. The first consisted of 17 female B6.*Sle1.2.3*: 4 mice of 3 months of age and 13 mice of 9–11 months of age. The aged mice were selected based on proteinuria test strips (Combur Test E, Roche): 6 mice with no or low proteinuria (<2) and 7 mice with high proteinuria (≥ 2). The second (time course) cohort consisted of 59 mice: 2 B6 mice (1 male and 1 female) and 8 B6.*Sle1.2.3* mice (4 male and 4 female, except at 10 months: 4 male and 3 female) each, sacrificed every 2 months from 2 to 12 months of age.

ELISA and colorimetric assays

Measurements of total IgG (Invitrogen, 88-50400) and anti-dsDNA IgG (Shibayagi, ARKDD-061) were performed according to manufacturers' protocols, on plasma diluted to fit onto standard curves. Results are expressed in $\mu\text{g}/\text{mL}$ and U/mL, respectively. Albumin concentration in urine was measured using the Mouse Albumin Matched Antibody Pair kit (Abcam ab210890). Briefly, 96-well high-binding plates were coated overnight at 4°C with 2 $\mu\text{g}/\text{mL}$ capture antibodies in a 35 mM NaHCO₃, 15 mM Na₂CO₃, pH 9.6 solution and blocked (1% BSA, 0.05% Tween 20 in PBS) for 2 hours at room temperature. Next, mouse albumin standards (from 12.5 ng/mL to 0.195 ng/mL) and urine samples (diluted in blocking buffer) were incubated on a shaker at 400 rpm for 2 hours at room temperature. Detection antibodies (0.5 $\mu\text{g}/\text{mL}$) were then added for 1 hour with shaking at room temperature, followed by 0.05 $\mu\text{g}/\text{mL}$ Streptavidin-HRP. Finally, TMB solution was added and the reaction stopped with H₂SO₄ 1N. Plates were washed three times with PBS-0.05% Tween 20 between each step. Optical density was measured at 490 nm with subtraction of background at 560 nm. Results are expressed in mg/dL. A mouse creatinine ELISA kit (Abcam, ab65340) was used on urine diluted to fit on the standard curve, following the manufacturer's protocol. Results are expressed in g/dL. Proteinuria was calculated as the urine albumin/creatinine ratio, expressed in mg of albumin per g of creatinine.

Immunofluorescence

IgG deposition was detected on 5 μm OCT serial kidney sections, with 1 $\mu\text{g}/\text{mL}$ anti-mouse IgG antibody coupled to AlexaFluor 488 (ThermoFisher, A-11001). Counterstaining was performed using 1 $\mu\text{g}/\text{mL}$ Hoechst 33342. Slides were digitalised on a Panoramic Confocal scanner (3DHitech) at $\times 20$ magnification. Glomeruli were scored from 0 (no IgG deposit) to 3 (severe IgG deposit). Values shown are the mean scores for 30 glomeruli from each kidney section, from three blinded scorers.

Senescence-associated β -galactosidase assay

Senescence-associated β -galactosidase (SA β -gal) assay was performed on 15 μm OCT serial kidney sections. Briefly, slides were fixed in 0.2% formaldehyde for 10 min. After

washing with PBS, slides were incubated with the staining solution (40 mM citric acid/Na phosphate pH 5.7, 5 mM $K_4[Fe(CN)_6] \cdot 3H_2O$, 5 mM $K_3[Fe(CN)_6]$, 150 mM NaCl, 2 mM $MgCl_2$, 1 mg/mL X-gal (Sigma-Aldrich, B4252)) overnight at 37°C in an incubator without CO_2 . Slides were then washed and counterstained 30s with haematoxylin. Slides were digitalised on a Panoramic Scan II scanner (3DHitech) at $\times 20$ magnification. A semi-quantitative score was given for 10–20 glomeruli per kidney section, with each glomerulus classified as moderate (1), intermediate (2) or high (3).

Histology and immunohistochemistry

Immunostaining with 1 μ g/mL anti-CD8 (Cell signalling, 98941S) and anti-p16^{Ink4a} (Abcam, ab211542), Picosirius red (PSR) and H&E staining were performed on 5 μ m FFPE serial kidney sections. PSR staining was performed as previously described.³⁴ Slides were digitalised on a Panoramic Scan II scanner (3DHitech) at $\times 20$ magnification. Computer-assisted quantification of p16^{Ink4a}-positive and CD8-positive cells over entire sections was performed using Author V.2017.2 (Visiopharm). Results shown are the number of p16^{Ink4a}-positive or CD8-positive cells per mm² of tissue. Semi-quantitative PSR staining scores (scale: 0–6) were obtained by adding the median glomerular fibrosis score and the median interstitial fibrosis score (absent: 0, low: 1, intermediate: 2, high: 3), from three blinded scorers. Activity and chronicity scores are median scores from three blinded scorers, based on H&E-stained kidney sections. Activity scores evaluate endocapillary proliferation, extracapillary proliferation, periglomerular and interstitial immune cell infiltration (each parameter scored between 0 and 3, total scale: 0–12). Chronicity scores evaluate glomerulosclerosis, thickness of fibrous tissue lining Bowman's capsules, tubular atrophy and interstitial fibrosis (each parameter scored between 0 and 3, total scale: 0–12).

Statistical analyses

Statistical analyses were performed on GraphPad Prism V.9.1.0: Mann-Whitney rank test for two-group comparisons, Kruskal-Wallis with Dunn's post-hoc tests for multiple-group comparisons, nested t-test for comparisons of subgroups within two groups and Spearman's rank-order correlation coefficient. Penetrance of disease parameters was calculated as: the percentage of mice displaying values above the mean plus 2 SD of values from all 12 (2–12 month old) B6 mice.

RESULTS

Cells positive for p16^{Ink4a}, a classic marker of cellular senescence, are observed in kidneys of aged B6.Sle1.2.3 lupus-prone mice

We conducted an exploratory study on a cohort of (n=17) female B6.Sle1.2.3 mice, to assess for the presence of

p16^{Ink4a}-positive cells in the kidney in this lupus-prone strain. Four mice of 3 months of age were included as pre-symptomatic controls; 13 mice of 9–11 months of age were selected based on urine protein estimated by dipstick, to capture kidney disease heterogeneity: 6 mice with low proteinuria (values: 0–1) and 7 with high proteinuria (values: ≥ 2). Quantitative measurement of proteinuria confirmed dipstick-based selection of the cohort: urine albumin/creatinine ratio was low in young mice (14.8–26.7 mg/g) and highly variable among aged mice (31.4–42702.1 mg/g) (online supplemental figure 1A), with a significant difference between the low (0–1) and high (2–3) dipstick groups (online supplemental figure 1B). Histopathological (activity and chronicity) scores also differed significantly between the low and high dipstick groups (online supplemental figure 1C,D), as did glomerular IgG deposition (online supplemental figure 1E). In contrast to kidney disease, systemic disease parameters (total IgG and anti-dsDNA antibody levels in plasma) were similar between the groups (online supplemental figure 1F,G), suggesting greater homogeneity of systemic autoimmunity.

As observed in samples from patient with LN,⁷ p16^{Ink4a} protein expression was highly variable among older mice: few p16^{Ink4a}-positive cells were detected in kidney sections of certain mice (illustrated in figure 1A, top left), comparable with kidneys from young mice (data not shown); others showed strong p16^{Ink4a} staining (illustrated in figure 1A, top right). Quantification of p16^{Ink4a} staining (p16^{Ink4a}-positive cells/mm²) confirmed this heterogeneity (range: 5.9–186.2, median: 42.2) (figure 1B). p16^{Ink4a}-positive cells were mainly observed in glomeruli, with staining of the glomerular tuft (containing endothelial cells, podocytes and mesangial cells) and strong positivity in Bowman's capsules (parietal epithelial cells) (figure 1C). Tubular cells and scattered cells in the tubulointerstitial compartment were also positively stained (figure 1C): a pattern similar to that observed in kidney biopsies from patients with LN.⁷ We performed an SA β -gal assay (a second widely used marker of cellular senescence) on frozen sections from low and high p16^{Ink4a}-positive kidneys (≤ 50 th vs > 50 th percentile, n=3 each). Semi-quantitative evaluation of glomerular β -gal staining showed that kidneys characterised by high p16^{Ink4a} displayed significantly higher glomerular β -gal scores than low p16^{Ink4a} kidneys (figure 1D,E). This suggests that cellular senescence is indeed detected in a proportion of aged B6.Sle1.2.3 mouse kidneys.

The presence of p16^{Ink4a}-positive cells is associated with renal disease severity in B6.Sle1.2.3 mice

We next asked whether p16^{Ink4a} is associated with kidney disease, assessed by several parameters: urine albumin/creatinine ratio, histopathology (activity, chronicity) scores and glomerular IgG deposits in kidney sections.

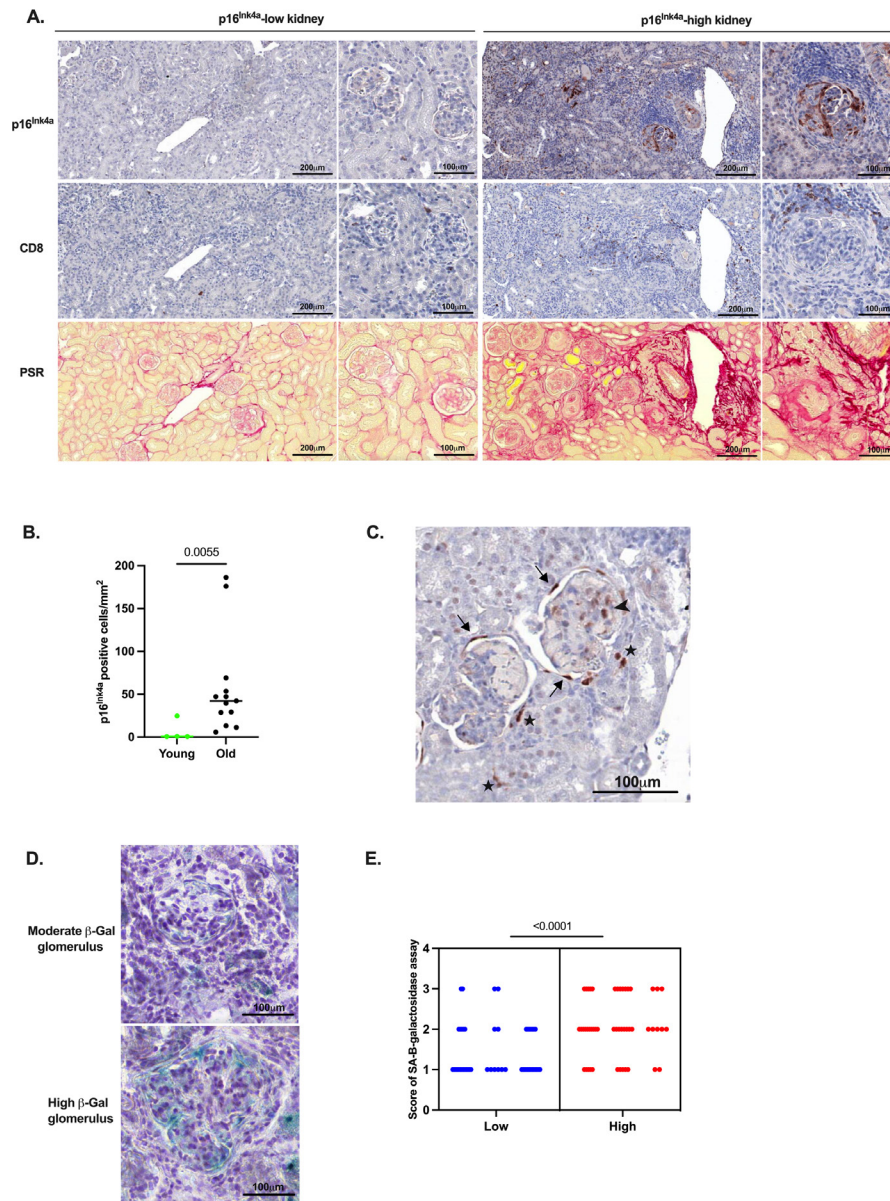


Figure 1 Markers of cellular senescence in kidneys from selected B6.Sle1.2.3 lupus-prone mice. (A) Anti-p16^{Ink4a} (top row), anti-CD8 (middle row) and Picrosirius red (PSR, bottom row) staining of FFPE kidney serial sections, from 2 mice of 10–11 months of age. Overview (scale: 200 μm) and close-up (scale: 100 μm) of a p16^{Ink4a}-low (≤50th percentile, left column) and a p16^{Ink4a}-high (>50th percentile, right column) example. (B) Quantification of p16^{Ink4a} (positive cells/mm²) in kidneys of 3 month-old mice (young; n=4) and 9–11 month-old mice (old; n=13). (C) Representative image from a kidney showing p16^{Ink4a}-positive cells on Bowman’s capsules (arrow), within glomeruli (arrowhead) and cells from tubulointerstitium (filled star). (D) Representative images and (E) semiquantitative scores of glomerular SA β-gal staining of frozen OCT sections from low (≤50th percentile, n=3) versus high (>50th percentile, n=3) p16^{Ink4a}-stained kidneys (10–20 glomeruli/mouse). Horizontal bars: medians. *p* values: Mann-Whitney test (p16^{Ink4a}), nested t-test (β-gal assay). B6.Sle1.2.3, B6.NZMSle1/Sle2/Sle3; FFPE, formalin-fixed paraffin-embedded; OCT, optimal cutting temperature; SA β-gal, senescence-associated β-galactosidase.

Mice with p16^{Ink4a}-high kidneys (upper 50th percentile: >Q2) displayed significantly higher urine albumin/creatinine ratios (figure 2A), as well as higher activity and chronicity scores (figure 2B,C). Accordingly, a significant positive correlation was observed between p16^{Ink4a} staining and urine albumin/creatinine ratios and activity and chronicity scores (figure 3A–C). Conversely, significantly lower glomerular IgG deposit scores were observed in p16^{Ink4a}-high kidneys (figure 2D); accordingly, a significant negative correlation was observed

between these values (figure 3D). This may reflect greater activation of renal cells, immune cell recruitment and (complement and Fc receptor-mediated) immune complex clearance leading, *in fine*, to greater tissue damage in mice with advanced kidney disease as compared with mice with mild kidney disease. In contrast to its correlation with kidney disease severity, p16^{Ink4a} was not associated with parameters of systemic disease such as total IgG and anti-dsDNA antibody levels in plasma (figure 2E,F).

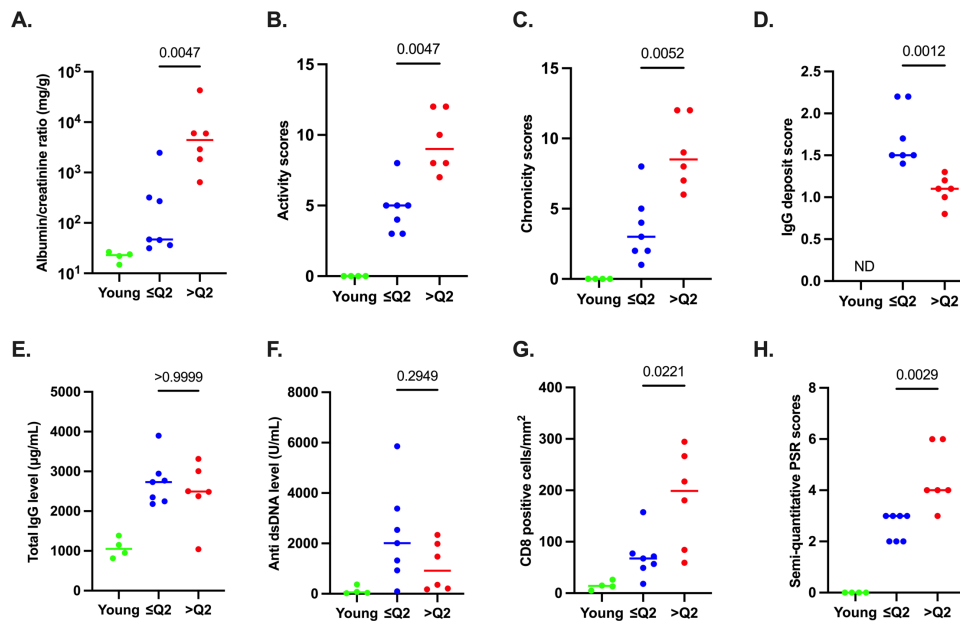


Figure 2 Association between $p16^{\text{Ink4a}}$ and renal disease in selected aged B6.Sle1.2.3 mice: 4 mice of 3 months of age (young), and 13 mice of 9–11 months of age with $p16^{\text{Ink4a}}$ -low (≤ 50 th percentile, $\leq Q2$) versus $p16^{\text{Ink4a}}$ -high (> 50 th percentile, $> Q2$) kidneys. (A–C) Renal disease parameters: urine albumin/creatinine ratio (mg/g), and histopathological activity and chronicity scores on H&E-stained FFPE kidney sections (scale: 0–12). (D) Semi-quantitative evaluation of glomerular IgG deposits in frozen OCT kidney sections. (E,F) Systemic disease parameters: total IgG ($\mu\text{g/mL}$) and anti-dsDNA antibody (U/mL) in plasma. (G,H) Quantification of anti-CD8 staining (positive cells/ mm^2) and semi-quantitative PSR staining scores (scale: 0–6) on serial FFPE kidney sections (with $p16^{\text{Ink4a}}$). Horizontal bars: medians. p values: Mann-Whitney test. anti-dsDNA, anti-double-stranded DNA; B6.Sle1.2.3, B6.NZMSle1/Sle2/Sle3; FFPE, formalin-fixed paraffin-embedded; ND, not determined; OCT, optimal cutting temperature; PSR, Picosirius red.

It has been shown that CD8^+ T lymphocytes are the predominant immune cell type infiltrating the LN kidney and that their presence is associated with renal disease severity.^{35–36} We previously showed a significant association between CD8^+ T cell infiltration, fibrosis and

$p16^{\text{Ink4a}}$ -positive cells in kidney biopsies of patients with LN.⁷ Sections (in series with those stained for $p16^{\text{Ink4a}}$) of mouse kidney were therefore stained for CD8^+ cells and with PSR for collagen fibres (figure 1A). Quantification showed that $p16^{\text{Ink4a}}$ -high biopsies displayed significantly

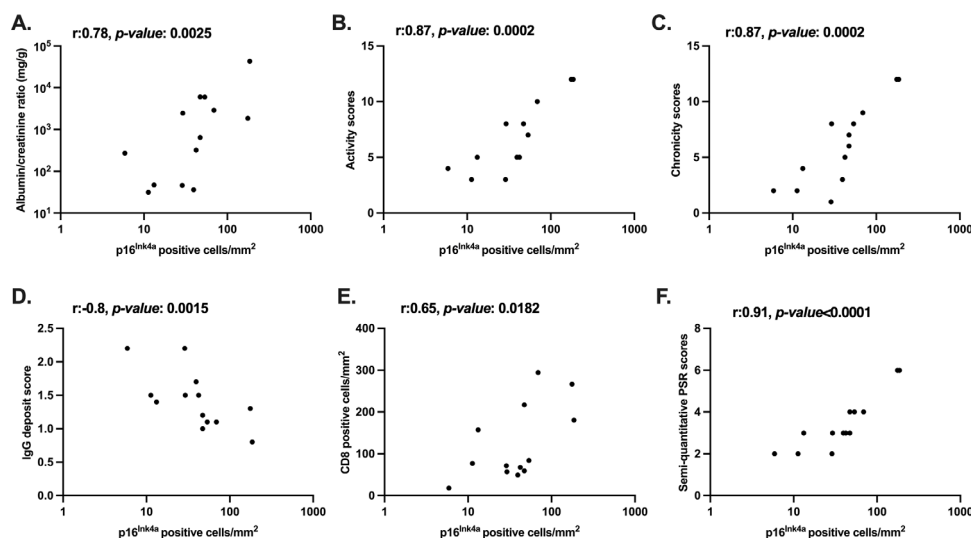


Figure 3 Correlation between kidney $p16^{\text{Ink4a}}$ staining, renal disease parameters and kidney CD8^+ T cell infiltration and fibrosis in aged B6.Sle1.2.3 mice. Correlation between $p16^{\text{Ink4a}}$ staining (positive cells/ mm^2) on FFPE kidney sections of 13 B6.Sle1.2.3 mice of 9–11 months of age, and (A) urine albumin/creatinine ratio (mg/g), (B,C) activity and chronicity scores (median from three blinded scorers, total scale: 0–12), (D) glomerular IgG deposit score (mean scores from three blinded scorers, 30 glomeruli/mouse), (E) CD8^+ T cell kidney infiltration (positive cells/ mm^2) and (F) renal fibrosis (semi-quantitative PSR staining scores, scale from 0 to 6). r and p values: Spearman's rank-order correlation coefficient. B6.Sle1.2.3, B6.NZMSle1/Sle2/Sle3; FFPE, formalin-fixed paraffin-embedded; PSR, Picosirius red.

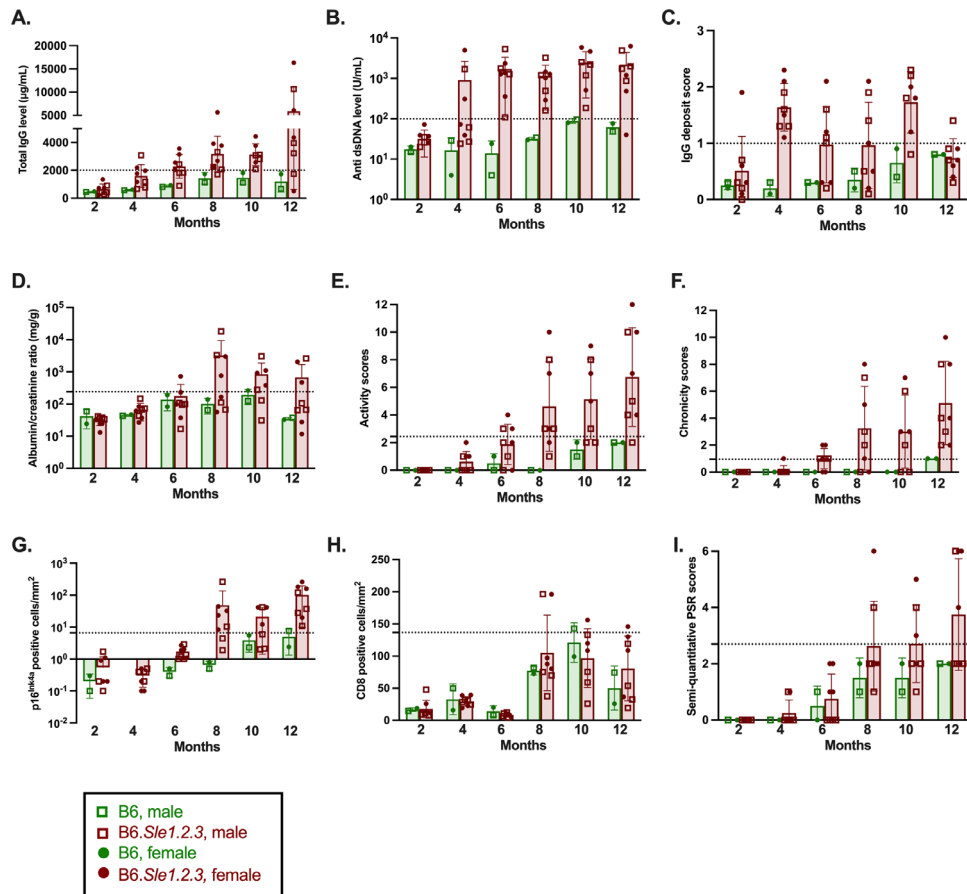


Figure 4 Disease parameters, kidney p16^{Ink4a}, CD8⁺ T cell infiltration and fibrosis over time. Two B6, 7 to 8 B6.Sle1.2.3 mice per time point. (A,B) Total IgG (µg/mL) and anti-dsDNA antibody (U/mL) in plasma. (C) Semi-quantitative evaluation of glomerular IgG deposits in frozen OCT kidney sections. (D) Urine albumin/creatinine ratio (mg/g). (E,F) Histopathological activity and chronicity scores on H&E-stained FFPE kidney sections (scale: 0–12). (G–I) Quantification of p16^{Ink4a} (positive cells/mm²), quantification of anti-CD8 staining (positive cells/mm²), semi-quantitative PSR staining scores (scale: 0–6) on serial FFPE kidney sections. Bars: mean±SD. Green: B6; maroon: B6.Sle1.2.3. Circles: female; squares: male. Horizontal dotted lines: mean plus 2SD of all 12 (2–12 month old) B6 mice. anti-dsDNA, anti-double-stranded DNA; B6.Sle1.2.3, B6.NZMSle1/Sle2/Sle3; FFPE, formalin-fixed paraffin-embedded; OCT, optimal cutting temperature; PSR, Picosirius red.

higher CD8⁺ T cell infiltration (figure 2G); they also showed significantly higher collagen deposition (with glomerulosclerosis, thickening of Bowman's capsules and interstitial fibrosis) as reflected by semi-quantitative scores of PSR staining (figure 2H). Accordingly, p16^{Ink4a} staining correlated positively with CD8⁺ T cell infiltration and with fibrosis (figure 3E,F).

Accumulation of p16^{Ink4a}-positive cells in B6.Sle1.2.3 kidneys occurs at 8 months of age, later than systemic disease and overlapping with renal disease

In order to study the temporal relationship between the appearance of p16^{Ink4a}, and systemic and renal disease parameters, we performed a time course in ageing mice. Two B6 controls and 8 B6.Sle1.2.3 lupus-prone mice were sacrificed at 2-month intervals, from 2 to 12 months of age. Penetrance of disease parameters (the percentage of B6.Sle1.2.3 mice displaying values above the mean plus 2SD of all 12 B6 mice) at the different time points is displayed in online supplemental figure 2. Systemic disease indices as well as glomerular IgG deposits appeared

in B6.Sle1.2.3 mice at 2–4 months of age (figure 4A–C and online supplemental figure 2A,B). Kidney disease became apparent later, with proteinuria (urine albumin/creatinine ratio) and histopathological scores rising from 6 months of age (figure 4D–F and online supplemental figure 2B). The appearance of p16^{Ink4a}-positive cells, CD8⁺ T cell infiltration and collagen deposition seemed to occur concurrently, at 8 months of age (figure 4G–I and online supplemental figure 2C). High penetrance (>50%) of glomerular IgG deposits and systemic disease parameters was observed at 4 and 6 months of age, respectively. In contrast, high penetrance of renal disease parameters (activity and chronicity scores, urine albumin/creatinine ratio) and p16^{Ink4a} occurred later, at 8 months of age. Finally, fibrosis (PSR staining) affected 50% of B6.Sle1.2.3 mice only by 12 months of age, while the peak penetrance of CD8⁺ T cell infiltration (at 8 months of age) was only 25% in B6.Sle1.2.3 mice (online supplemental figure 2C).

In order to assess for whether p16^{Ink4a}, once it appeared at 8 months of age, was indeed associated with kidney

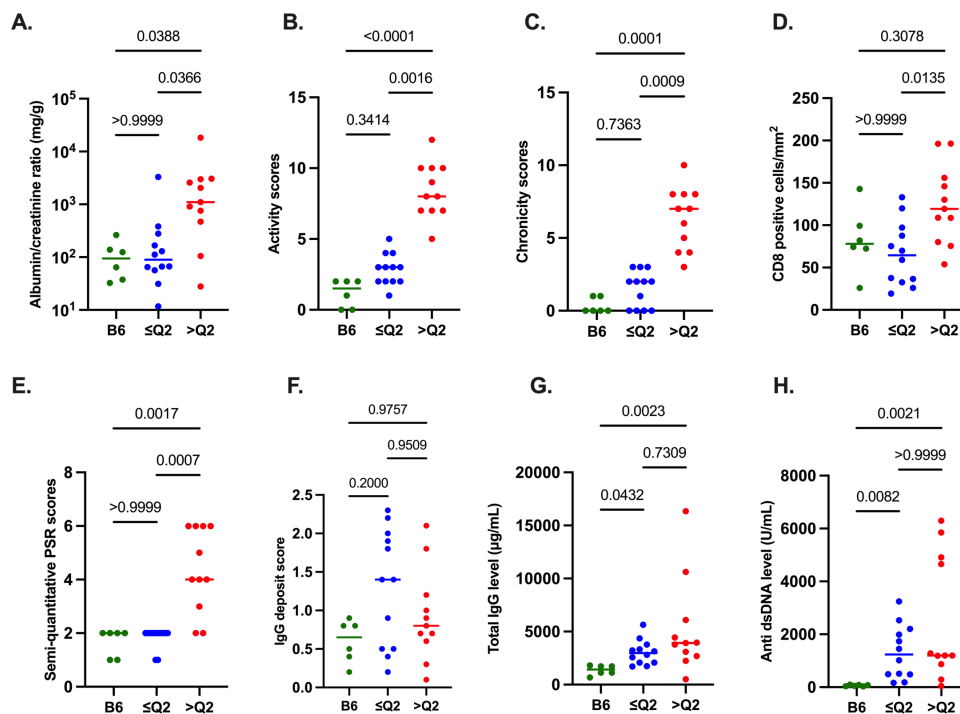


Figure 5 Association of p16^{Ink4a} staining with renal disease in a second (ageing) cohort: 8–12 month-old mice (6 B6, 23 B6.*Sle1.2.3* mice). (A–C) Renal disease parameters: urine albumin/creatinine ratio (mg/g), histopathological activity and chronicity scores on H&E-stained FFPE kidney sections (scale: 0–12). (D,E) Quantification of anti-CD8 staining (positive cells/mm²) and semi-quantitative PSR staining scores (scale: 0–6) on serial FFPE kidney sections (with p16^{Ink4a}). (F) Semiquantitative evaluation of glomerular IgG deposits in frozen OCT kidney sections. (G,H) Systemic disease parameters: total IgG (μg/mL) and anti-dsDNA antibody (U/mL) in plasma. Horizontal bars: medians. *p* values: Kruskal-Wallis and Dunn's post-hoc tests. $\leq Q2$: p16^{Ink4a}-low (≤ 50 th percentile), $> Q2$: p16^{Ink4a}-high (> 50 th percentile) B6.*Sle1.2.3* kidneys. anti-dsDNA, anti-double-stranded DNA; B6.*Sle1.2.3*, B6.*NZMSle1/Sle2/Sle3*; FFPE, formalin-fixed paraffin-embedded; OCT, optimal cutting temperature; PSR, Picosirius red.

disease in this second cohort, we pooled data from the mice 8–12 months old. Aged B6.*Sle1.2.3* mice in the upper 50th percentile ($> Q2$) for p16^{Ink4a} staining showed significantly higher renal disease scores, CD8⁺ T cells and PSR scores, than those in the lower 50th percentile ($\leq Q2$; figure 5A–E). Indeed, the $\leq Q2$ p16^{Ink4a} B6.*Sle1.2.3* group did not differ significantly from B6 on renal disease parameters and fibrosis, whereas the $> Q2$ p16^{Ink4a} group did (figure 5A–E). Glomerular IgG deposits did not differ significantly between groups (figure 5F). Finally, systemic disease scores (total IgG and dsDNA antibody levels in plasma) did not differ between the $\leq Q2$ and $> Q2$ p16^{Ink4a} B6.*Sle1.2.3* groups, and were higher in both as compared with B6 (figure 5G,H). Together, this suggests that in the context of (relatively consistent) systemic autoimmune insult to the kidney, the cellular senescence marker p16^{Ink4a} may be useful in flagging (highly heterogeneous) renal disease in B6.*Sle1.2.3* mice.

DISCUSSION

We demonstrate for the first time, in two separate cohorts of B6.*1.2.3* mice, that high kidney p16^{Ink4a} staining, a major hallmark of cellular senescence, is significantly associated with increased proteinuria, histopathological scores, CD8⁺ T cell infiltration and renal fibrosis. In contrast, p16^{Ink4a} positivity is not associated with systemic

disease parameters (nor with age and sex; data not shown). This recapitulates observations made in patients with LN.⁷ Immunohistochemistry for the detection of p16^{Ink4a} protein, a CDK inhibitor (*CDKN2A*) responsible for cell cycle arrest during cellular senescence, is widely used to assess cellular senescence *ex vivo*. The upregulation of β -galactosidase activity, another hallmark of cellular senescence, was confirmed in a small subset of mice by a colorimetric enzymatic test (SA β -galactosidase assay), used to detect cellular senescence in fresh/frozen material *ex vivo* and *in vitro*.¹¹

Whether cellular senescence participates in kidney disease progression, or is simply a consequence (and potentially useful marker), remains to be determined. A detrimental effect of senescent cells may be exerted through the profibrotic, proinflammatory secretome (SASP) typical of senescent cells.^{12–13} While the SASP is particularly suited to engaging the immune system (including CD8⁺ T lymphocytes)^{14–19} for the clearance of senescent cells, the latter can upend the process by inhibiting cytolytic cells.^{18–19} It has been suggested that persistence of senescent cells (due to the overwhelming or inhibition of the immune response) tips the balance from a positive to a negative impact. Senescence may also contribute to disease by rendering renal cells functionally incompetent. Renal progenitor cells (RPCs), a subset

of parietal epithelial cells on the Bowman's capsule, are strongly p16^{Ink4a} stained in B6.*Sle1.2.3* mice: a pattern also observed in human samples.⁷ Where healthy RPCs would be able to regenerate glomerular and tubular structures thanks to their capacity to proliferate and differentiate into renal cell subsets,^{37–39} their senescence may hamper tissue repair.^{40 41}

Interestingly, the selective elimination of senescent cells (in *Ink4a*^{-/-} mice or the *Ink4a*-ATTAC model) was shown to relieve fibrotic lesions and improve renal function in ageing and allograft survival.^{42 43} The study of cellular senescence may thus provide a therapeutic opportunity in LN, complementary to current, largely immune-directed tools. In this context, the first open-label pilot studies using the senolytic drugs dasatinib plus quercetin have shown promising results in patients with idiopathic pulmonary fibrosis and diabetic kidney disease.^{44 45} We performed a time course, designed to guide future studies testing senolytic therapies in the B6.*Sle1.2.3* lupus model. We found that while systemic disease parameters appear at 4 months and show consistently high penetrance over time, kidney disease becomes overt later (from 6 to 8 months of age based on this small ageing cohort) and is more variable. In keeping with incomplete renal disease penetrance, mortality in our colony was also lower than originally reported (100% by 12 months of age³³): 30–40% at 10 months, 50% by 12 months and >80% at 18 months of age (values based on our entire colony; data not shown).

Because p16^{Ink4a} is not detected prior to other signs of kidney disease, it is as yet unclear whether cellular senescence actually contributes to tissue injury in this model; it may well be a consequence of pathogenic processes such as activation of complement, activation of renal cells and recruitment of pro-inflammatory cells.² Multiple pro-inflammatory factors including interferon- β have indeed been implicated in cellular senescence induction.^{46 47} Further experiments will be therefore required in order to demonstrate a role of cellular senescence in pathogenesis.

The B6.*Sle1.2.3* triple congenic strain spontaneously develops autoimmunity akin to human SLE,^{33 48} making it an attractive choice in which to model disease. The ability of senolytic therapy to delay renal disease onset or ameliorate its severity in the context of systemic autoimmunity in this model would provide strong support for a pathogenic role of cellular senescence in LN.

Acknowledgements We acknowledge Professor Anabelle Decottignies and Dr Bernard Lauwerys for valuable scientific discussions.

Contributors GT and ED contributed equally to this paper. GT, ED, LW, CAB, DN, FB, FL and AD performed experiments and analysed data. CB analysed data, reviewed and edited the manuscript. GT and NL wrote the manuscript. GT, ED, SL and NL conceived the study, reviewed and edited the manuscript. NL is responsible for the overall content as the guarantor.

Funding This work was supported by Fonds de la Recherche Scientifique (FNRS, under grant no. CDR J.0124.22), Actions de Recherche Concertées, UCLouvain (A.R.C. grant 19/24–098) and unrestricted grants from Cap48 (RTBF). NL is a chercheur qualifiée de the FNRS.

Competing interests None declared.

Patient and public involvement Patients and/or the public were not involved in the design, or conduct, or reporting, or dissemination plans of this research.

Patient consent for publication Not required.

Ethics approval This study was approved by the Ethics Committee of Université catholique de Louvain (2018/UCL/MD/37). All experiments were conducted with full compliance with local, national, ethical, and regulatory principles and local licensing regulations.

Provenance and peer review Not commissioned; externally peer reviewed.

Data availability statement Data are available upon reasonable request.

Supplemental material This content has been supplied by the author(s). It has not been vetted by BMJ Publishing Group Limited (BMJ) and may not have been peer-reviewed. Any opinions or recommendations discussed are solely those of the author(s) and are not endorsed by BMJ. BMJ disclaims all liability and responsibility arising from any reliance placed on the content. Where the content includes any translated material, BMJ does not warrant the accuracy and reliability of the translations (including but not limited to local regulations, clinical guidelines, terminology, drug names and drug dosages), and is not responsible for any error and/or omissions arising from translation and adaptation or otherwise.

Open access This is an open access article distributed in accordance with the Creative Commons Attribution Non Commercial (CC BY-NC 4.0) license, which permits others to distribute, remix, adapt, build upon this work non-commercially, and license their derivative works on different terms, provided the original work is properly cited, appropriate credit is given, any changes made indicated, and the use is non-commercial. See: <http://creativecommons.org/licenses/by-nc/4.0/>.

ORCID iD

Nisha Limaye <http://orcid.org/0000-0002-9820-4794>

REFERENCES

- Hahn BH. Antibodies to DNA. *N Engl J Med* 1998;338:1359–68.
- Maria NI, Davidson A. Protecting the kidney in systemic lupus erythematosus: from diagnosis to therapy. *Nat Rev Rheumatol* 2020;16:255–67.
- Hanly JG, O’Keeffe AG, Su L, et al. The frequency and outcome of lupus nephritis: results from an international inception cohort study. *Rheumatology (Oxford)* 2016;55:252–62.
- Dall’Era M, Cisternas MG, Smilek DE, et al. Predictors of long-term renal outcome in lupus nephritis trials: lessons learned from the Euro-lupus nephritis cohort. *Arthritis Rheumatol* 2015;67:1305–13.
- Tamirou F, Lauwerys BR, Dall’Era M, et al. A proteinuria cut-off level of 0.7 G/day after 12 months of treatment best predicts long-term renal outcome in lupus nephritis: data from the MAINTAIN nephritis trial. *Lupus Sci Med* 2015;2:e000123.
- Vandepapelière J, Aydin S, Cosyns J-P, et al. Prognosis of proliferative lupus nephritis subsets in the Louvain lupus nephritis inception cohort. *Lupus* 2014;23:159–65.
- Tilman G, Bouzin C, Aydin S, et al. High P16Ink4A, a marker of cellular senescence, is associated with renal injury, impairment and outcome in lupus nephritis. *RMD Open* 2021;7:e001844.
- HAYFLICK L, MOORHEAD PS. The serial cultivation of human diploid cell strains. *Exp Cell Res* 1961;25:585–621.
- Serrano M, Lin AW, McCurrach ME, et al. Oncogenic Ras provokes premature cell senescence associated with accumulation of P53 and P16Ink4A. *Cell* 1997;88:593–602.
- Campisi J, d’Adda di Fagagna F. Cellular senescence: when bad things happen to good cells. *Nat Rev Mol Cell Biol* 2007;8:729–40.
- Dimiri GP, Lee X, Basile G, et al. A biomarker that identifies senescent human cells in culture and in aging skin in vivo. *Proc Natl Acad Sci U S A* 1995;92:9363–7.
- Coppé J-P, Desprez P-Y, Krtolica A, et al. The senescence-associated secretory phenotype: the dark side of tumor suppression. *Annu Rev Pathol* 2010;5:99–118.
- Hernandez-Segura A, Nehme J, Demaria M. Hallmarks of cellular senescence. *Trends Cell Biol* 2018;28:436–53.
- Xue W, Zender L, Miething C, et al. Senescence and tumour clearance is triggered by P53 restoration in murine liver carcinomas. *Nature* 2007;445:656–60.
- Krizhanovsky V, Yon M, Dickins RA, et al. Senescence of activated stellate cells limits liver fibrosis. *Cell* 2008;134:657–67.
- Kang T-W, Yevsa T, Woller N, et al. Senescence surveillance of pre-malignant hepatocytes limits liver cancer development. *Nature* 2011;479:547–51.

- 17 Iannello A, Thompson TW, Ardolino M, *et al.* P53-dependent chemokine production by senescent tumor cells supports Nkg2D-dependent tumor elimination by natural killer cells. *J Exp Med* 2013;210:2057–69.
- 18 Pereira BI, Devine OP, Vukmanovic-Stejic M, *et al.* Senescent cells evade immune clearance via HLA-E-mediated NK and Cd8(+) T cell inhibition. *Nat Commun* 2019;10:2387.
- 19 Wang T-W, Johmura Y, Suzuki N, *et al.* Blocking PD-L1-PD-1 improves senescence surveillance and ageing phenotypes. *Nature* 2022;611:358–64.
- 20 Chkhotua AB, Gabusi E, Altamari A, *et al.* Increased expression of P16(Ink4A) and P27(Kip1) Cyclin-dependent kinase inhibitor genes in aging human kidney and chronic allograft nephropathy. *Am J Kidney Dis* 2003;41:1303–13.
- 21 Melk A, Schmidt BMW, Takeuchi O, *et al.* Expression of P16Ink4A and other cell cycle regulator and senescence associated genes in aging human kidney. *Kidney Int* 2004;65:510–20.
- 22 Sis B, Tasanarong A, Khoshjou F, *et al.* Accelerated expression of senescence associated cell cycle inhibitor P16Ink4A in kidneys with glomerular disease. *Kidney Int* 2007;71:218–26.
- 23 Westhoff JH, Hilgers KF, Steinbach MP, *et al.* Hypertension induces somatic cellular senescence in rats and humans by induction of cell cycle inhibitor P16Ink4A. *Hypertension* 2008;52:123–9.
- 24 Verzola D, Gandolfo MT, Gaetani G, *et al.* Accelerated senescence in the kidneys of patients with type 2 diabetic nephropathy. *Am J Physiol Renal Physiol* 2008;295:F1563–73.
- 25 Liu J, Yang J-R, He Y-N, *et al.* Accelerated senescence of renal tubular epithelial cells is associated with disease progression of patients with immunoglobulin A (IgA) nephropathy. *Translational Research* 2012;159:454–63.
- 26 Yang C, Xue J, An N, *et al.* Accelerated glomerular cell senescence in experimental lupus nephritis. *Med Sci Monit* 2018;24:6882–91.
- 27 Rieux-Laucat F, Le Deist F, Hivroz C, *et al.* Mutations in Fas associated with human lymphoproliferative syndrome and autoimmunity. *Science* 1995;268:1347–9.
- 28 Fisher GH, Rosenberg FJ, Straus SE, *et al.* Dominant interfering Fas gene mutations impair apoptosis in a human autoimmune lymphoproliferative syndrome. *Cell* 1995;81:935–46.
- 29 Drappa J, Vaishnav AK, Sullivan KE, *et al.* Fas gene mutations in the canale-Smith syndrome, an inherited lymphoproliferative disorder associated with autoimmunity. *N Engl J Med* 1996;335:1643–9.
- 30 Mohan C, Alas E, Morel L, *et al.* Genetic dissection of SLE pathogenesis. Sle1 on murine chromosome 1 leads to a selective loss of tolerance to H2A/H2B/DNA Subnucleosomes. *J Clin Invest* 1998;101:1362–72.
- 31 Mohan C, Morel L, Yang P, *et al.* Genetic dissection of systemic lupus erythematosus pathogenesis: Sle2 on murine chromosome 4 leads to B cell hyperactivity. *J Immunol* 1997;159:454–65.
- 32 Mohan C, Yu Y, Morel L, *et al.* Genetic dissection of SLE pathogenesis: Sle3 on murine chromosome 7 impacts T cell activation, differentiation, and cell death. *J Immunol* 1999;162:6492–502.
- 33 Morel L, Croker BP, Blenman KR, *et al.* Genetic reconstitution of systemic lupus erythematosus immunopathology with polycongenic murine strains. *Proc Natl Acad Sci U S A* 2000;97:6670–5.
- 34 Courtoy GE, Leclercq I, Froidure A, *et al.* Digital image analysis of picosirius red staining: a robust method for multi-organ fibrosis quantification and characterization. *Biomolecules* 2020;10:1585.
- 35 Couzi L, Merville P, Deminière C, *et al.* Predominance of Cd8+ T lymphocytes among periglomerular infiltrating cells and link to the prognosis of class III and class IV lupus nephritis. *Arthritis Rheum* 2007;56:2362–70.
- 36 Pamfil C, Makowska Z, De Groof A, *et al.* Intrarenal activation of adaptive immune effectors is associated with tubular damage and impaired renal function in lupus nephritis. *Ann Rheum Dis* 2018;77:1782–9.
- 37 Bussolati B, Bruno S, Grange C, *et al.* Isolation of renal progenitor cells from adult human kidney. *Am J Pathol* 2005;166:545–55.
- 38 Sagrinati C, Netti GS, Mazzinghi B, *et al.* Isolation and characterization of multipotent progenitor cells from the Bowman's capsule of adult human kidneys. *J Am Soc Nephrol* 2006;17:2443–56.
- 39 Lazzeri E, Ronconi E, Angelotti ML, *et al.* Human urine-derived renal progenitors for personalized modeling of genetic kidney disorders. *J Am Soc Nephrol* 2015;26:1961–74.
- 40 Molofsky AV, Slutsky SG, Joseph NM, *et al.* Increasing P16Ink4A expression decreases forebrain progenitors and neurogenesis during ageing. *Nature* 2006;443:448–52.
- 41 Golomb L, Sagiv A, Pateras IS, *et al.* Age-associated inflammation connects RAS-induced senescence to stem cell dysfunction and epidermal malignancy. *Cell Death Differ* 2015;22:1764–74.
- 42 Braun H, Schmidt BMW, Raiss M, *et al.* Cellular senescence limits regenerative capacity and allograft survival. *J Am Soc Nephrol* 2012;23:1467–73.
- 43 Baker DJ, Childs BG, Durik M, *et al.* Naturally occurring P16(Ink4A)-Positive cells shorten healthy lifeSpan. *Nature* 2016;530:184–9.
- 44 Justice JN, Nambiar AM, Tchkonja T, *et al.* Senolytics in idiopathic pulmonary fibrosis: results from a first-in-human, open-label, pilot study. *EBioMedicine* 2019;40:554–63.
- 45 Hickson LJ, Langhi Prata LGP, Bobart SA, *et al.* Senolytics decrease senescent cells in humans: preliminary report from a clinical trial of dasatinib plus quercetin in individuals with diabetic kidney disease. *EBioMedicine* 2019;47:446–56.
- 46 Moiseeva O, Mallette FA, Mukhopadhyay UK, *et al.* DNA damage signaling and P53-dependent senescence after prolonged beta-interferon stimulation. *Mol Biol Cell* 2006;17:1583–92.
- 47 Acosta JC, Banito A, Wuestefeld T, *et al.* A complex secretory program orchestrated by the inflammasome controls paracrine senescence. *Nat Cell Biol* 2013;15:978–90.
- 48 Celhar T, Fairhurst AM. Modelling clinical systemic lupus erythematosus: similarities, differences and success stories. *Rheumatology (Oxford)* 2017;56(suppl_1):i88–99.